International Journal of Computer Assisted Radiology and Surgery (2018) 13:905–916
https://doi.org/10.1007/s11548-018-1769-8

ORIGINAL ARTICLE

RF-ablation pattern shaping employing switching channels of dual bipolar needle electrodes: ex vivo results

Jens Ziegle[1] · Chloé Audigier[2] · Johannes Krug[1] · Ghazanfar Ali[1] · Younsu Kim[2] · Emad M. Boctor[2] · Michael Friebe[1]

Received: 29 January 2018 / Accepted: 13 April 2018 / Published online: 20 April 2018

Abstract

Purpose Radiofrequency (RF) ablation with mono- or bipolar electrodes is a common procedure for hepatocellular carcinoma (HCC) with a low rate of recurrence for small size tumors. For larger lesions and/or non-round/ellipsoid shapes RF ablation has some limitations and generally does not achieve comparable success rates to microwave ablation or high-intensity focused ultrasound therapies.

Materials and methods To shape RF ablations for matching a tumor size and geometry, we have developed an electronic channel switch box for two bipolar needles that generates multiple selectable ablation patterns. The setup can be used with commercially available mono- or bipolar RF generators. The switch box provides ten selectable ablation procedures to generate different ablation patterns without a relocation of a needle. Five patterns were exemplary generated in ex vivo tissue of porcine liver and chicken breast and visually characterized.

Results Different ablation patterns, e.g., in a L- or U-shape, were achieved. In chicken breast a maximum ablation with a diameter of 4.3 cm was obtained and in porcine liver 2.8 cm with electrodes of 0.9 cm length.

Conclusion The resulting ablations with the electronic switch box and two bipolar needles show the potential ability to manage RF therapies of complex and large tumor geometries. Next steps would be to validate the actual tissue ablation volumes in further ex vivo and preclinical studies and against simulation results.

Keywords Ablation pattern · Bipolar RF needle · Radiofrequency ablation · RFA · Thermal therapy · Tumor ablation

Introduction

Non-resectable hepatocellular carcinoma (HCC) is commonly treated by ablation, i.e., using radiofrequency, microwave, high-intensity focused ultrasound, ethanol ablation or cryoablation. The most common is radiofrequency ablation (RFA), which is performed by a percutaneous insertion of a needle electrode to produce coagulative necrosis of the tumor with alternating current. For HCC smaller than 3 cm, RFA achieves treatment success rates comparable to conventional resection methods [1,2]. It has been shown that the recurrence rate for tumor sizes ≤ 2.5 cm is about 21.6 % and increases for larger tumor sizes, e.g., about 52.8 % for tumor of 2.6 cm $-$ 4.0 cm and 68.8 % for $>$ 4.1 cm [3]. In some cases of RFA interventions, the optimal alignment of a single needle to the tumorous tissue is obscured by bones, other organs or vessels. Therefore, another entry point needs to be chosen which may not be the optimal solution to ablate the whole tumor at once. A tumor can also have a complex geometry, and multiple needles or multiple relocations of a single needle have to be applied to achieve a matching ablation pattern. In particular, a therapy for complex metastases structure in bone has a need of better selectable ablation patterns [4].

To treat complex and/or large tumor geometries a combination of three or more electrodes is needed, but this procedure application also includes a higher degree of invasiveness. Multiple relocations (even more than twice) of a single needle have to be performed under image guidance,

✉ Jens Ziegle
jens.ziegle@ovgu.de

Chloé Audigier
caudigi1@jhmi.edu

[1] Department of Medical Engineering, Otto-von-Guericke University, Magdeburg, Saxony-Anhalt, Germany

[2] Department of Computer Science, Johns Hopkins University, Baltimore, MD, USA

which extend the time of the intervention and, eventually, destroy more healthy tissue. In RFA therapy, no system is currently available that allows an individual combination of selectable electrodes [5] to manipulate the ablation pattern.

To overcome that problem and take advantage of the relatively simple clinical procedure, we propose to perform RFA with two bipolar needles whose four electrodes can be combined individually. This allows to adjust the direction of ablation through the lesion even in a non-optimal position without a relocation of a single needle.

In this paper, we introduce a developed electronic switch box that allows to select the ablation pathways between two bipolar needles. The switch box interconnects one output of a RF generator to the four electrodes of two bipolar needles. Using the switch box for controlling the electrode's channel outputs, different ablation pathways can be generated between two electrodes at once. The selection of these electrodes for the RF output current determines the orientation and direction of the ablation zone. Therefore, a variety of ablation patterns with only two bipolar needles can be generated to match complex tumor geometries. We evaluate the performance of the switch box in an experimental setup by generating different ablation patterns in ex vivo chicken breast and porcine liver tissues. We compare the ablation results that are performed by a commonly used monopolar and regular bipolar RF generator in combination with our switch box. We measure and qualify the obtained ablations into three zones—necrotic, coagulated and transitional zone.

Background

Percutaneous RFA is a widely used method to treat various types of tumors or malignant diseases by means of tissue heating. For that, one or more RFA needles containing one or more electrodes are placed inside or near the tumor. Monopolar and bipolar ablation systems exist. In monopolar systems, a needle with a single electrode is placed into the tumorous lesion, whereas the counter electrode is placed on the patient's skin using a large, adhesive electrode. For bipolar systems, both electrodes are on the needle itself. A high-frequency alternating current (AC) oscillates between these electrodes with a steady frequency in the range of 200 kHz and 1200 kHz [6]. The conductive surrounding tissue completes the electric circuit, and consequently, the AC flow creates ionic agitation and frictional heating within the tissue. The heat generated by the electrical current spreads into the surrounding tissue until a thermal equilibrium is reached [7,8], and extracellular and intracellular water is driven out of the tissue which results into coagulation and further into tissue destruction (necrosis) [9].

The amount of heat produced at a certain location between the electrodes depends on various factors such as electric current density, impedance/resistance of the tissue, thermal capacity, thermal conduction, blood supply and others. A temperature increase above 60 °C in tissue usually leads to a successful ablation [10]. The bioheat equation developed by Pennes describes the heating of tissue considering the heating source as well as electrical and physiological tissue characteristics [11].

To increase the ablation volume, the electrical power and/or procedure duration needs to be increased. However, this causes larger current densities close to the electrodes which can result in faster necrosis and, hence, in a rapidly increasing impedance. Once the impedance exceeds a certain threshold, no further ablation is possible [12,13].

The volume and shape of the ablation zone is mainly defined by a certain needle design or by the placement of various combined needles. Using various (bipolar) needles inside or around the tumor allows to generate larger ablation volumes. Shaping the ablation zones is however limited by the hardware and the needles provided by the manufactures. In currently available systems, the user has no control on the electrical current that is applied between the electrodes of different RF needles.

Materials and methods

RF switch box

A relay-based switch box was developed to provide an interface between the output of a monopolar or bipolar RF generator and the electrodes of two bipolar RF needles, and the schematic of the switch box is shown in Fig. 1a. The two output channels of a bipolar RF generator or the RF signal channel and ground channel of a monopolar RF generator are connected to the switch box inputs. There are four relays for each of the two input channels. Four are used to switch between RF signal and disconnection and four to switch between ground and disconnection. The used relays are electromagnetic types with a maximum supportive AC voltage of 440 V and a maximum applicable power of 384 W. The switch box has four output channels, one for each electrode of the two bipolar needles. The relays are triggered by an 8-bit AVR (Atmega328P-PU) microcontroller which is connected to an user interface (UI), see Fig. 1b. Ten predefined procedures, see Fig. 2, and the procedure time in minutes can be selected. Each of these procedures generates a different ablation pattern. The first six procedures generate vertical, horizontal and diagonal patterns. The RF power is selected at the RF generator. Starting an ablation procedure with the switch box enables the input channels. The actual ablation begins by pressing the RF generator start button or pedal. The switch box recognizes the RF signal input and activates the output channels. The output channels are switched according

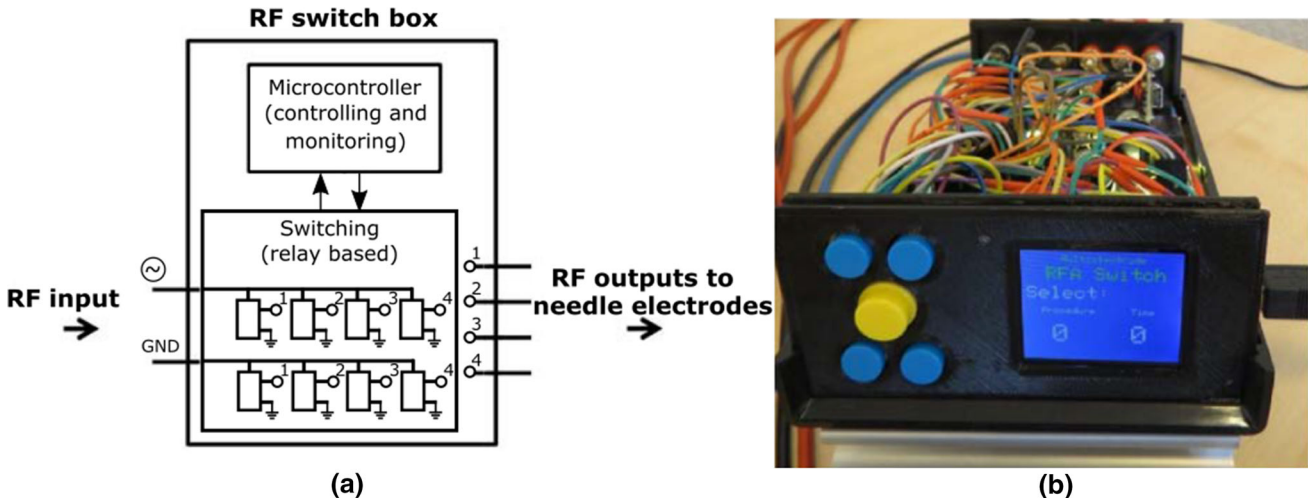

Fig. 1 Switch box routing the output of a RF generator to four different electrodes using relays (**a**). The relays switch the four outputs between RF signal, ground and disconnection using a microcontroller. Each output channel addresses one electrode of two bipolar needles. Predefined ablation procedures with defined pattern generation can be selected via the user interface (**b**)

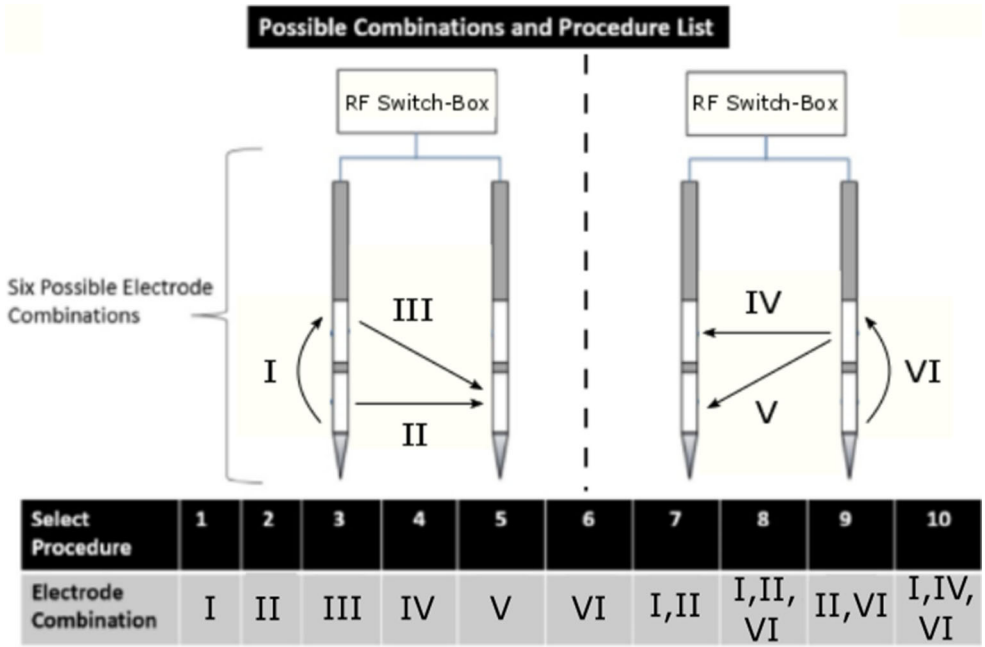

Select Procedure	1	2	3	4	5	6	7	8	9	10
Electrode Combination	I	II	III	IV	V	VI	I,II	I,II, VI	II,VI	I,IV, VI

Fig. 2 Predefined ablation procedures with different electrode combinations. Depending on the selected procedure, a different ablation pattern is generated. L- or U-shaped patterns are generated by consecutive combination of the first six procedures. Two different L-shapes (7 and 9) and one U-shape (8 and 10) are initially implemented in the switch box. More patterns can be added by programming the microcontroller

to the selected procedure, i.e., two of the needle's electrodes are active and two are disconnected. A consecutive combination of the first six procedures is used to generate more complex patterns like L- and U-shapes that are programmed in procedure 7 to 10, e.g., a U-shaped pattern is generated by an automatic consecutive selection of two vertical plus one horizontal ablation as shown in Fig. 3a. The selected procedure time is applied for each ablation direction. More patterns, e.g., like in Fig. 3b, c, can be added by programming the microcontroller. After the selected procedure duration elapses, the switch box will disconnect the input from the output channels by switching off the relays—the RF generator is then automatically deactivated. For the change of the ablation direction, which is needed to achieve a L- or U-shape, the output channels are switched by the relays and a new electrode pair is selected. While switching the channels, the

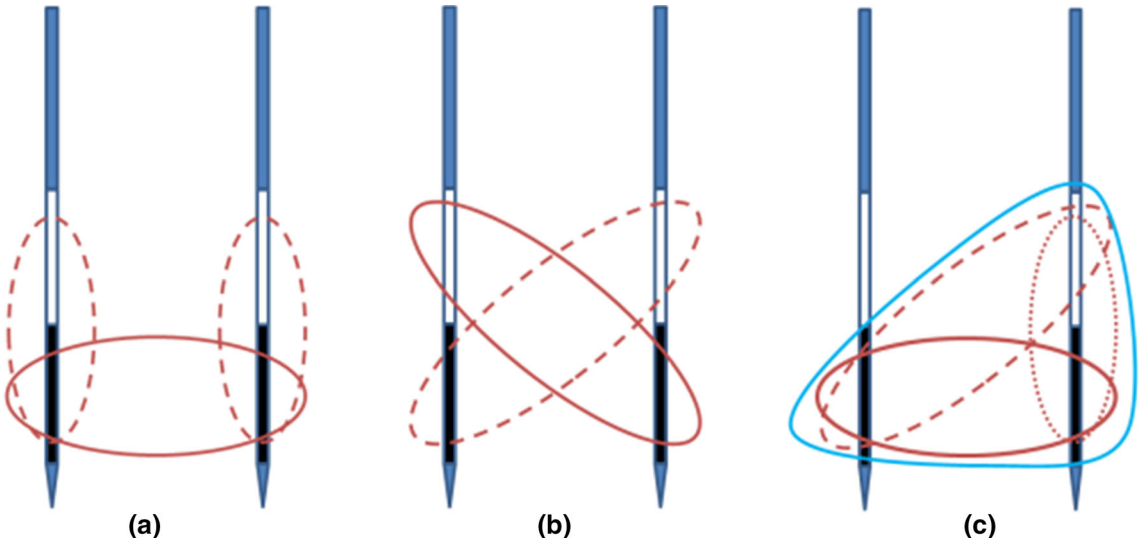

Fig. 3 Two bipolar needle setup with electrodes (black and white parts) to realize a U-shaped ablation pattern (**a**) by the combination of vertical (dashed line) and horizontal (solid line) selection. For a L-shaped ablation pattern any vertical and horizontal pattern can be combined. Selection of two different diagonal-shaped patterns (**b**). Triangular-shaped pattern by the combination of diagonal-, horizontal- and vertical-shaped pattern (**c**)

RF signal has no connection to the electrodes for a very short time. Within this short time, the RF generator recognizes this signal breakdown as an infinitely high impedance and stops the RF signal output immediately. To overcome this mechanism, the generator's start button or pedal is locked in its 'on' position. Therefore, after a new electrode pair is selected, the generator recognizes an impedance in its working range and continues the RF signal.

Experimental setup

Setup with bipolar RF generator

Figure 4a shows the experimental setup with the bipolar RF generator (CelonLab POWER, Olympus Surgical Technologies Europe, Hamburg, Germany) that provides a maximum power output of 250 W and a RF signal with $< 275\,V_p$ and frequency of 470 kHz $\pm$ 10 kHz. Its power control system uses the effective resistance of the tissue instead of tissue impedance and is working with a load resistance between 15 Ω and 900 Ω. The two RF generator outputs of one bipolar needle were connected to the switch box, first and second RF output to the first and second switch box input, respectively. Two bipolar needles (CelonProSurge 150-T20, Olympus Surgical Technologies Europe, Hamburg, Germany) with a total length of 150 mm and a diameter of 1.8 mm were connected to the switch box output. At its tip, the needle has two 9-mm-long electrodes with a spacing of 2-mm insulating material. The needles were used in combination with a water cooling system (CelonAquaflow *III*, Olympus Surgical Technologies Europe, Hamburg, Germany) with a flow rate of 30 ml/min, and two of its three available cooling pumps were used simultaneously. The cooling reduces the heat at the electrode material and therefore helps to avoid fast tissue carbonization.

Setup with monopolar RF generator

Figure 4b shows the monopolar RF generator (Radionics RF Cool-Tip, Medtronics, Minneapolis, MN, USA). The monopolar RF generator provides impedance-based and manual power control with a maximum power output of 200 W for a working load between 10 Ω and 1000 Ω. The RF signal has an output voltage of $< 260\,V_p$ with a frequency of 480 kHz $\pm$ 10%. In both power control settings the system stops delivering energy if the impedance is not in the range of the defined working load. With the impedance-based control mode, the energy delivery continues automatically after the impedance recovers into the range of the working load. The RF signal channel and the grounding pad channel were used as input to the RF switch box. In this case, one electrode of the two bipolar needles always serves as RF signal and the other electrode as ground. Therefore, the current flow spreads along the electric field from generator electrode to the electrode that is connected to the ground. In this sense, the monopolar RF generator was used in a bipolar fashion. Two bipolar needles (CelonProSurge 150-T20, Olympus Surgical Technologies Europe, Hamburg, Germany) were attached to the output channels of the switch box. A water cooling system (Masterflex Cooling Drive, Barnant, Barrington, IL, USA), see Fig. 4c, provided the two bipolar needles with cooling

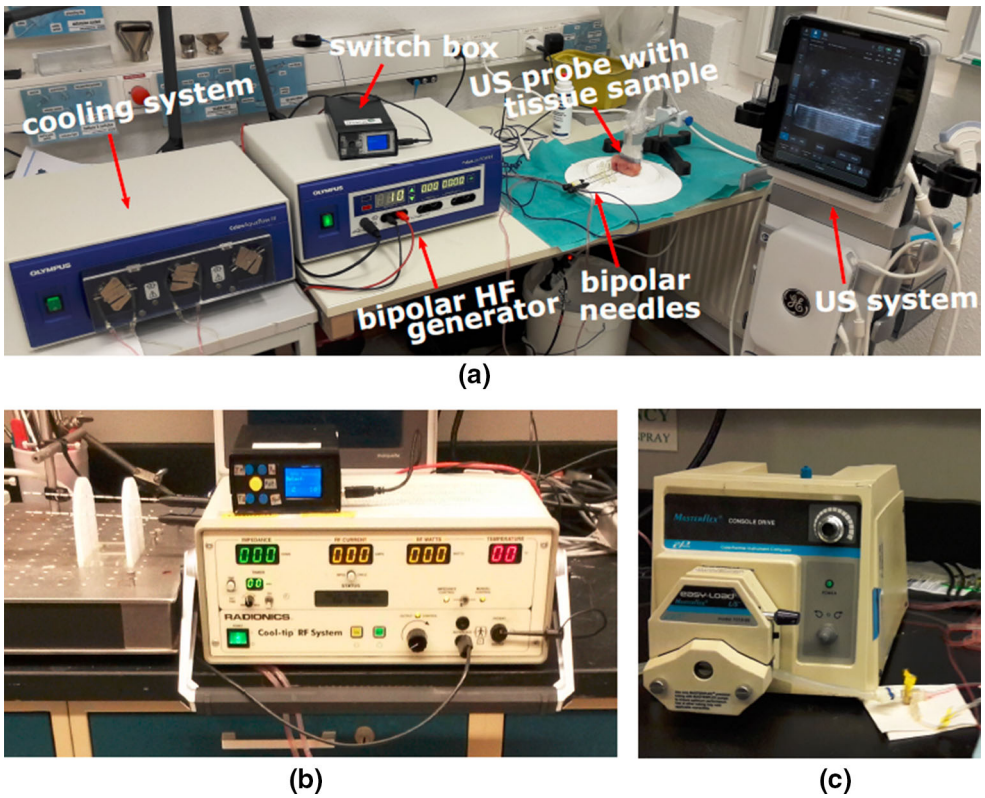

Fig. 4 Experimental setup with CelonAquaflow *III* water cooling system, bipolar CelonLab *POWER* RF generator and RF switch box on top, CelonProSurge 150-T20 bipolar needles, tissue sample with GE 12L-SC 4-13 MHz Linear Probe attached to GE Venue 50 (**a**). Setup with Radionics RF Cool-Tip monopolar RF generator with two CelonProSurge 150-T20 bipolar needles and RF switch box (**b**) in combination with Masterflex Cooling Drive system (**c**)

water with a flow rate of about 60 ml/min at a pump speed setting of 8.0.

Experimental protocol

Needle placement

For both generator setups, the bipolar needles were placed parallel with the help of two stencils that were included in the needle package. Each stencil provided a insertion pitch of 20, 30 and 40 mm between two needles. The stencils were interconnected at the 40-mm pitch holes using screws, see Fig. 5a. The 20-mm pitch was used to insert the needles into the tissue until the whole electrode parts were covered. The same insertion depth for both needles was verified by existing equidistant color rings on the bipolar needles indicating a pitch of 10 mm for each of them. This setup was chosen for the reproducibility of the experiments. An US imaging system (Venue 50, 12L-SC 4-13 MHz Linear Probe, General Electric, GE Healthcare) was used for insertion guidance inside liver tissue to avoid a placement inside vessel structures.

Ablation in ex vivo tissue

In both RF generator setups, the ex vivo chicken breast and porcine liver were maintained at room temperature of 23 °C during the ablation procedures. Overall, ten pieces each of chicken breast and 20 pieces of porcine liver were used for each of the two RF generator setups. The volume of the ex vivo chicken breast varied between 64 and 96 cm^3 and for the porcine liver between 80 and 112 cm^3.

Ablation patterns with an U- or L-shape as well as diagonal and horizontal shapes between the two bipolar needles were generated as initial tests of the switch box system with the mono- and bipolar RF generator system. Also, a vertical ablation pattern along one bipolar needle was generated. The vertical ablations generated with the bipolar RF generator setup in chicken breast and porcine liver were used as references of standard bipolar RF ablation.

For the generation of an U-shaped ablation, three different ablation directions were applied. This was achieved by the selection of procedure number 8 at the switch box, see Fig. 2. Therefore, the corresponding electrode pairs were consecutively switched and the ablation time was applied for each direction. In the experiments, the resistance-based

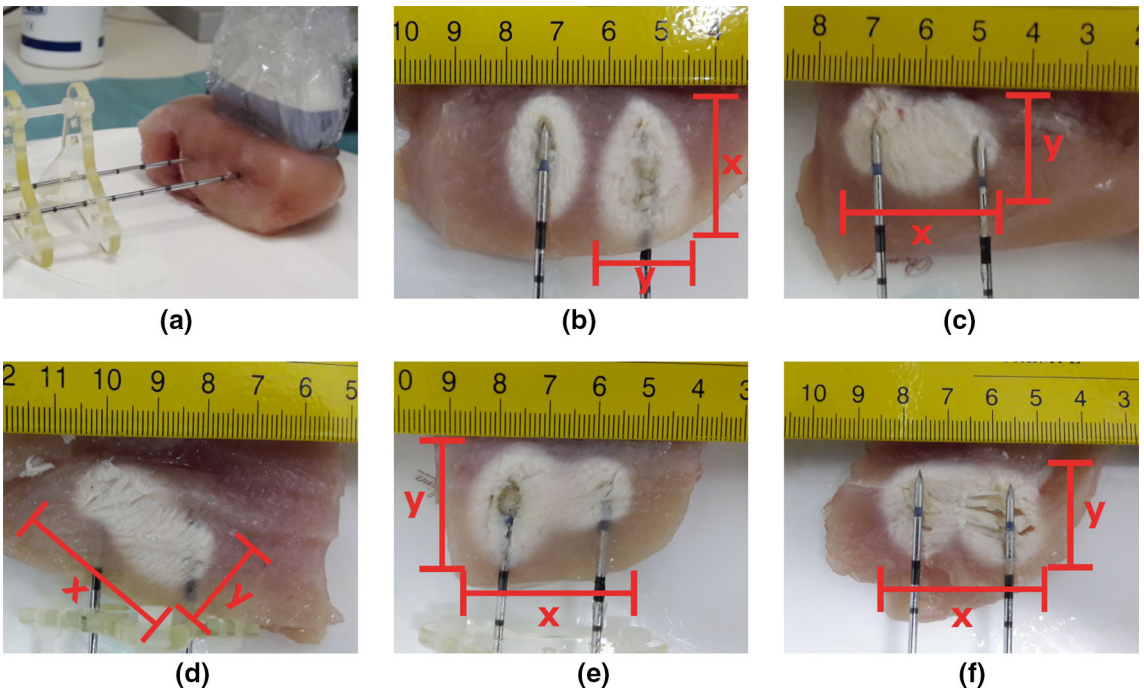

Fig. 5 Images of the needle and US probe placement in chicken breast (**a**) and ablation zone of vertical (**b**), horizontal (**c**), diagonal (**d**), L-shaped (**e**) and U-shaped (**f**) patterns, generated by using bipolar RF generator setup. Red bars indicate the measuring lines along the maximum length (x) and width (y) of the ablation zone

Table 1 Parameter settings of the RF generators (power) and the switch box (ablation procedure and duration) for ablations in chicken breasts

Ablation		Bipolar setup		Monopolar setup	
Pattern	Procedure	Power [W]	Duration [min]	Power [W]	Duration [min]
Vertical	1	20	4	10	8
Horizontal	2	20	4	10	8
Diagonal	3	20	4	10	8
L-shape	9	20	8	10	16
U-shape	8	20	12	10	24

Table 2 Parameter settings of the RF generators (power) and the switch box (ablation procedure and duration) for ablations in porcine liver

Ablation		Bipolar setup		Monopolar setup	
Pattern	Procedure	Power [W]	Duration [min]	Power [W]	Duration [min]
Vertical	1	40	6	10	8
Horizontal	2	40	6	10	8
Diagonal	3	40	6	10	8
L-shape	9	40	12	10	16
U-shape	8	40	18	10	24

power control was used for the bipolar RF generator and the impedance-based power control was used for the monopolar RF generator. The experiment parameters for the switch box (ablation procedure and time) and the RF generators (power) are listed in Table 1 for the chicken breast and in Table 2 for the porcine liver.

Measurement of ablation sizes

The ablated tissue volumes were axially cut along the needle path, where the largest ablation zone was expected to be visible, while the needles were still in place. A ruler was placed next to the ablation area and images were taken. A conversion factor was calculated for every image using the number

Table 3 Measurements of ablation zones in chicken breast generated with the bipolar RF setup with the maximum reached power. Maximum ablation length and maximum width in comparison with the standard bipolar reference ablation (vertical), given in percent

Pattern	Max. power (W)	Max. length x [mm](%)	Max. width y [mm](%)
Vertical	16	33.5 (ref.)	24.9 (ref.)
Horizontal	17	33.6 (+0.3)	21.3 (− 14.5)
Diagonal	20	34.3 (+2.4)	19.5 (− 21.7)
L-shape	16	30.5 (−8.9)	20.7 (− 16.9)
U-shape	19	43.5 (+29.9)	25.2 (+1.2)

of pixels appropriate to a 10-mm scale on the depicted ruler to report the measurements in the millimeter scale. Profiles in the images were taken using the software ImageJ (version 1.51), and a pixel intensity change along the profiles was used to visually identify the border between coagulated and healthy tissue. These borders were used to measure the maximum length and width of each ablation pattern. The length was always set as the biggest diameter of the ablation zone and the width as the biggest diameter perpendicular to it. All sizes of the generated ablations were compared to the respective size of the reference ablation.

In the images of the chicken breast ablations, the maximum length and width of a visible change to the normal tissue were measured in pixel and converted to millimeter with the corresponding calculated conversion factor.

In the images of the porcine liver ablations, the whole area of changed tissue color was categorized into three zones; (I) necrotic/carbonized zone, adjacent to the electrode, (II) coagulated zone, further away from the electrode, and (III) transitional zone as the outer visible layer. In the literature, the area inside a macroscopically visible hemorrhagic rim adjacent to the normal hepatic tissue corresponds to irreversible cell damage due to histological assessments of in vivo specimens [14]. The hemorrhagic rim is accounted as the transitional zone, and thus, cells within this margin, i.e., in coagulated and necrotic/carbonized zones, are accounted as areas of successful ablation. Therefore, the size of successful ablation was restricted to the edge of the coagulated zone, see Fig. 7b. Maximal width and length of the successful ablation were measured in pixel and converted to millimeter with the corresponding calculated conversion factor.

Results

Ablations in chicken breast: bipolar RF setup

Figure 5b shows two reference ablation patterns that were generated by each single bipolar needle in a standard way of a procedure. The ablation patterns resulted in ellipsoid shapes along the vertical direction of the needles. A maximum coagulation length (x) of 33.5 mm and maximum width (y) of 24.9 mm in the axial plane, i.e., along the needles, were achieved. Every generated ablation pattern between the needle electrodes (horizontal, diagonal, L- and U-shaped) resulted in a connected coagulation, see Fig. 5c–f. The maximum length and width of the different ablation zones are listed in Table 3. The horizontal and L-shaped (Fig. 5c, e) ablation procedures resulted in coagulations with butterfly shapes between the needle tips. All ablation procedures except for the L-shape managed to reach at least the same length as in the reference ablation pattern. The L-shaped ablation was 3 mm less in length and therefore 8.9% shorter.

Ablations in chicken breast: monopolar RF setup

A single bipolar needle ablation pattern, i.e., vertical along the two electrodes of one needle, could hardly be generated, see Fig. 6a. Its maximum length was 7.3 mm and maximum width was 6.2 mm, that is − 78.2 and − 75.1 %, respectively, smaller than the standard bipolar reference ablation. Ablation procedures between the two bipolar needles were successfully performed. The horizontal and diagonal ablation patterns were generated, as shown in Fig. 6b, c, with maximum ablation length of 28.1 and 37.8 mm, respectively—see Table 4. The maximum length of the horizontal ablation pattern is about 16.3% smaller compared to the same pattern generated with the bipolar RF generator setup. In the diagonal ablation process, it was about 10.2% larger. Ablation procedures with vertical ablation directions, i.e., L- and U-shaped patterns, could not be generated.

Ablations in porcine liver: bipolar RF setup

The ablation zones are shown in Fig. 7. The procedure with the horizontal as well as the L-shaped pattern resulted in a butterfly shape of the coagulated zone, as shown in Fig. 7a, e, respectively. In the standard single bipolar ablation procedure, i.e., vertical ablation (Fig. 7c), a coagulated zone with a maximum length of 12.8 mm and width of 10.0 mm was generated. The generated maximum lengths of the horizon-

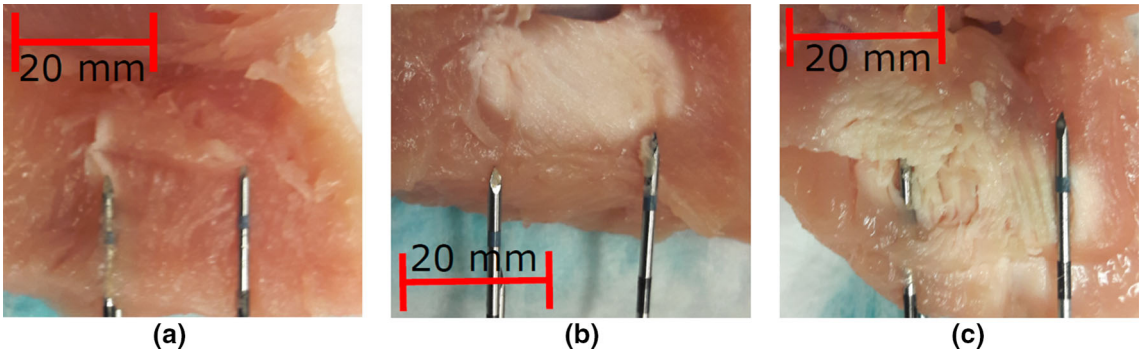

Fig. 6 Ablation zones in chicken breast with vertical (**a**), horizontal (**b**) and diagonal (**c**) shape generated by using the monopolar RF generator setup. Red bars indicate the scale for the measurements

Table 4 Measurements of ablation zones in chicken breast generated with the monopolar RF setup with the maximum reached power. Maximum ablation length and maximum width in comparison with the standard bipolar reference ablation, given in percent

Pattern	Max. power [W]	Max. length x [mm](%)	Max. width y [mm](%)
Vertical	7	7.3 (− 78.2)	6.2 (− 75.1)
Horizontal	8	28.1 (− 16.1)	17.8 (− 28.5)
Diagonal	10	37.8 (+ 12.8)	20.3 (− 18.5)
L-shape	–	–	–
U-shape	–	–	–

tal, L- and U-shaped patterns were all larger compared to the vertical ablation. The diagonal pattern showed no interconnected coagulation zone between the addressed electrodes, see Fig. 7d. The measured length and width for the different ablation patterns in porcine liver are listed in Table 5. The largest coagulated zone was created by the U-shaped procedure with a maximum length of 43.5 mm and maximum width of 25.2 mm that are 121.9% and 118.0% larger than in the standard bipolar reference ablation.

Ablations in porcine liver: monopolar RF setup

The achieved maximum power per procedure and ablation lengths and widths are listed in Table 6. Vertical ablation patterns could not be generated with the monopolar RF generator setup, see Fig. 8a. Thus, L- and U-shaped ablation patterns were not possible to achieve. The diagonal ablation procedure resulted in a coagulated zone with 7.1 mm length besides a large transitional zone between the needles, see Fig. 8b.

Discussion

In this study, we presented an additional low-cost device for monopolar and bipolar RF-ablation therapy systems that enables the generation of distinct ablation patterns. Using the presented RF switch box device in combination with a commercial RF generator allows the usage of two bipolar RF needles with only one RF generator output. Initial experiments with 5 different patterns in ex vivo chicken breast and porcine liver tissues confirmed the capability of achieving distinct ablation shapes from selectable ablation pathways. The most replicable results with our switch box were achieved in combination with the bipolar RF generator.

The ablation zones within the chicken breast (see Fig. 5) actually show the capability of generating complete and almost even distributed coagulations between two bipolar needles using the presented switch box system with the bipolar RF setup. All selected procedures generated the expected ablation patterns which demonstrate a correct functioning of the switch box with the bipolar RF generator. With the monopolar RF generator setup, the RF power had to be reduced because of the fast increase in tissue impedance of chicken breast. If the impedance went high in a short period of time, the system switched off the power. For that reason, the power was reduced to a maximum of 10 W for the chicken breast. Therefore, ablation duration was increased up to 8 min. One reason could be the presence of tissue structures, like cartilage in chicken breast, which impede the current flow between the electrodes. Another reason could be fast generated necrosis at the electrode with the RF signal altering the conductivity of the surrounding tissue. Since a vertical ablation procedure was not successfully achieved with the needle configuration used in the experiment, L- and U-shaped ablation patterns could also not be generated. The

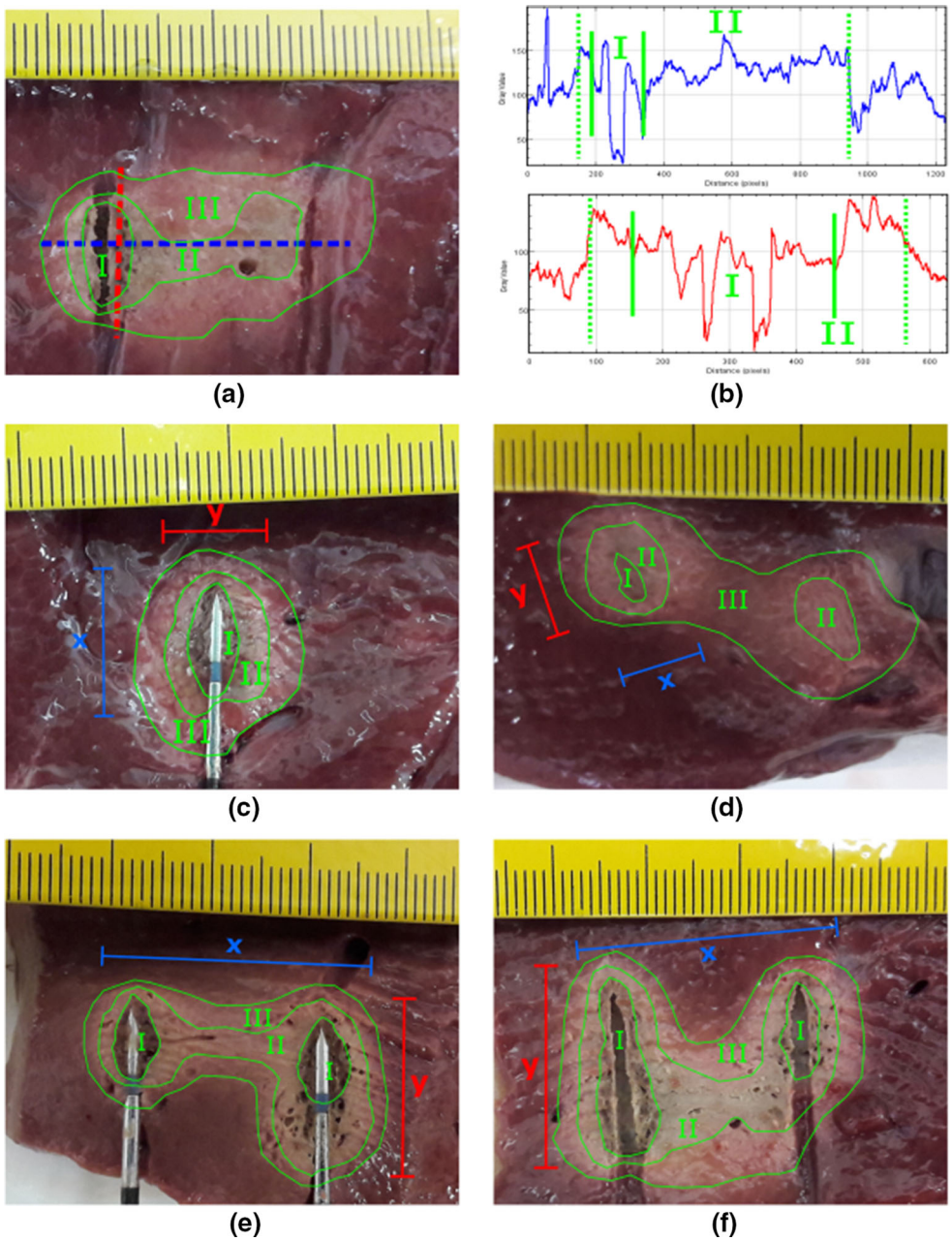

Fig. 7 Ablation zones in porcine liver tissues of horizontal pattern **a** with example profile used for ablation size measurements. **b** Along the profiles for length (x) in blue and width (y) in red limited to the coagulated zone (II). Each ablation is categorized in necrotic/carbonized (I), coagulated (II) and transitional zone. Ablation zones of vertical (**c**), diagonal (**d**), L-shaped (**e**) and U-shaped (**f**) patterns. All patterns were generated by using the bipolar RF generator setup in combination with the switch box

chicken breasts used in the experiments were different in size but also in tissue density and had probably different water content as well. This could have affected the size of the ablation zones since the RF generators also automatically adjust the output power according to the measured tissue resistance.

The ablations in liver tissue had to be implemented twice for each ablation pattern. Initial settings of maximum 20 W power resulted in incomplete coagulations between the bipolar needles, and no ablation length could be measured and therefore a power of 40 W was used instead. A higher-power settings for the RF signal helped to generate a fully coagulated zone between the two electrodes. Some coagulated zones had butterfly shapes that are stated as not clinically usable due to its uneven distribution of coagulation [5]. This behavior makes it difficult to predict the ablation shape, and

Table 5 Measurements of ablation zones in porcine liver generated with the bipolar RF setup with the maximum reached power. Maximum ablation length and maximum width in comparison with the standard bipolar reference ablation (vertical), given in percent

Pattern	Max. power [W]	Max. length *x* [mm](%)	Max. width *y* [mm](%)
Vertical	36	12.8 (ref.)	10.0 (ref.)
Horizontal	34	21.7 (+67.2)	8.9 (− 11.0)
Diagonal	36	− (−)	6.0 (− 40.0)
L-shape	33	27.6 (+115.6)	17.3 (+73.0)
U-shape	37	28.4 (+121.9)	21.8 (+118.0)

Table 6 Measurements of ablation zones in porcine liver generated with the monopolar RF setup with the maximum reached power. Maximum ablation length and maximum width in comparison with the standard bipolar reference ablation, given in percent

Pattern	Max. power [W]	Max. length *x* [mm](%)	Max. width *y* [mm](%)
Vertical	10	5.3 (− 58.6)	4.2 (− 58.0)
Horizontal	–	–	–
Diagonal	7	7.1 (− 44.5)	–
L-shape	–	–	–
U-shape	–	–	–

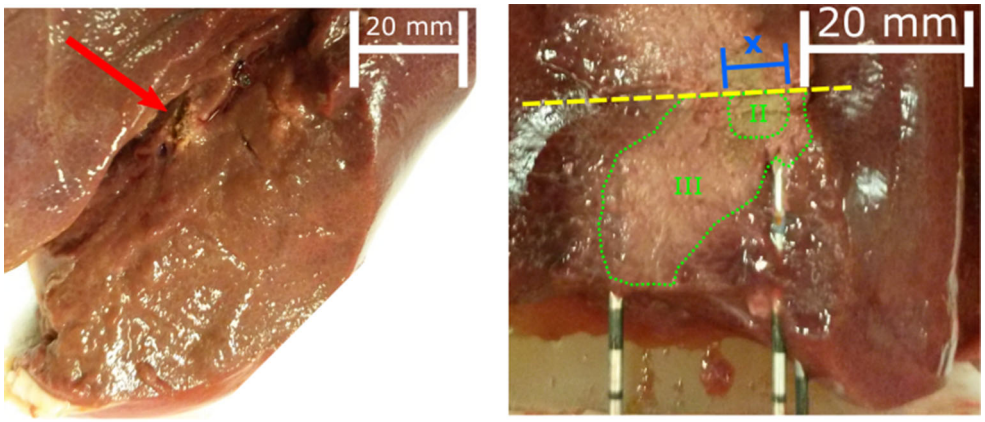

Fig. 8 Ablation patterns generated in porcine liver with the use of a monopolar RF generator setup in combination with the switch box. The arrow in **a** points to an incomplete vertical ablation along two electrodes on a bipolar needle. In the diagonal ablation pattern **b** a coagulated zone (II) is visible on the top of the right needle, and a measurement of length was taken. The dashed line indicates the end of the tissue layer cut. Between the two needles there was a large transitional zone (III) generated

therefore, its application would complicate the intervention planning. In this case, a higher-power setting could have increased the probability of generating a complete coagulation. In comparison with the ablations in the chicken tissue, the ablation patterns in liver were not always generated as expected. The tissue structure in liver is complex due to present blood vessels and bile ducts, and this can influence the current flow between the electrodes. The tissue of the chicken breast has less complex structures, and therefore, the generation of a pathway for the induced current flow is less complicated. Complete ablation patterns in liver tissue could also be generated by adjusting the RF power and/or RF duration settings.

For the more complex patterns, electrodes were addressed twice for a change in the ablation direction which caused a repeated heat induction between these electrodes. In these cases, it can become problematic if the tissue gets necrotic, and therefore, the electrical conductivity between the needle and the tissue would decrease and the ablation procedure might be stopped by the RF generator. This could alter the quality of ablation and prolong the procedure duration. But, there was no breakdown during the conduction of the exper-

iments. It has to be checked also in the case where higher power (> 40 W) for the monopolar RF generator signal is used.

The ablation generation using a monopolar RF generator in combination with the presented RF switch box needs to be improved. For example, it has to be checked whether using the manual power control instead of impedance-based control can improve the ablation generation. Further, the parallel placement of the needle in the presented experimental protocol may not always be applicable in a clinical application. Needles may be aligned further away or narrower to each other with some anti-parallel alignment. This may cause a difference in the ablation pattern geometry due to a changed electrical pathways between the electrodes. This change could also be controlled by observing the needle positions using image guidance. Also, tests with prolonged ablation duration or higher RF power need to be implemented to show which settings are needed to generate a complete and even distributed coagulation between two needles in combination with the presented switch box.

Since each ablation pattern was only realized once for initial tests, further tests are required to obtain results which are statistically more relevant. In the presented experiments a lower RF power setting was used to avoid fast impedance increase by heat because no perfusion was present, which helps to partially transfer heat out of the ablation zone. In contrary, for experiments in the literature with perfused ex vivo liver samples, the RF power is set starting from 60 to 80 W and is increased up to 130 to 150 W within a duration of maximum 21 min [14,15] which is comparable to the clinical application. The experimental setup can be improved to approach the outcomes expected in clinical intervention. Controlling the temperature of the sample tissue up to 37 °C to mimic body temperature would help to have a more realistic tissue behavior, regarding, e.g., tissue impedance, heat capacity and electric current distribution. Additionally, an artificial perfusion within the liver can be added to mimic blood flow which would add the function of partial heat sink. A study to obtain the full coagulated volume needs to be implemented in the near future for predictive quality assessment. A study with a tissue mimicking phantom for RFA application [16,17] could help to identify the whole ablation volume for different electrode sizes of bipolar RF needles and different ablation patterns. Using these improvements, a more clinically relevant outcome of ablation generation with the switch box can be achieved.

The knowledge of the ablation direction due to our system can be used in simulations to obtain a heat map of the ablation zone using biophysical modeling [18] and using time-of-flight change in ultrasound caused by the ablation [19]. An estimated heat map can support the physician at the crucial decision-making time and therefore improve the treatment's success.

Conclusion

The presented evaluation of our RF switch box gives an initial impression of the capability of controlling the ablation direction to generate complex and user-defined ablation pattern. Our system enables the opportunity to overcome needle placement restriction by adjusting the direction of ablation, and it can help to spare healthy tissue by matching the ablation to the tumor geometry. It could also be used for bone tumor application, e.g., in spine, which has more complex tumor geometries. A combination of computational estimation of ablation extent with the control of ablation direction can improve the planning of RF interventions. Thus, a precise treatment of individual tumor geometries can be achieved and their recurrence rate would therefore be decreased.

Acknowledgements Equipment for this study was partly provided by the Olympus Winter & Ibe GmbH of the Olympus Surgical Technologies Europe.

Compliance with ethical standards

Conflict of Interest The authors declare that they have no conflict of interest.

Human and animal rights This article does not contain any studies with human participants or animals performed by any of the authors. This article does not contain patient data.

References

1. Liu H, Wang Z-G, Fu S-Y, Li A-J, Pan Z-Y, Zhou W-P, Lau W-Y, Wu M-C (2016) Randomized clinical trial of chemoembolization plus radiofrequency ablation versus partial hepatectomy for hepatocellular carcinoma within the Milan criteria. Br J Surg 103:348–356
2. Potretzke TA, Ziemlewicz TJ, Hinshaw JL, Lubner MG, Wells SA, Brace CL, Agarwal P, Lee FT (2016) Microwave versus radiofrequency ablation treatment for hepatocellular carcinoma: a comparison of efficacy at a single center. J Vasc Interv Radiol 27:631–638
3. Kuenzli BM, Abitabile P, Maurer CA (2011) Radiofrequency ablation of liver tumors: actual limitations and potential solutions in the future. World J Hepatol 3:8–14
4. Proschek D, Tonak M, Zangos S, Mack M, Kurth A (2012) Radiofrequency ablation in experimental bone metastases using a controlled and navigated ablation device. J Bone Oncol 1:63–66
5. Mulier S, Jiang Y, Wang C, Jamart J, Marchal G, Michel L, Ni Y (2012) Bipolar radiofrequency ablation with four electrodes: ex vivo liver experiments and finite element method analysis. Influence of inter-electrode distance on coagulation size and geometry. Int J Hyperth 28:686–697
6. Wong K-P, Lang BH-H (2013) Use of radiofrequency ablation in benign thyroid nodules: a literature review and updates. Int J Endocrinol 2013, Article ID 428363
7. Goldberg SN (2001) Radiofrequency tumor ablation: principles and techniques. Eur J Ultrasound 13:129–147
8. Strasberg S, Linehan D (2003) Radiofrequency ablation of liver tumors. Curr Probl Surg 40:459–498

9. Minami Y, Kudo M (2011) Radiofrequency ablation of hepatocellular carcinoma: a literature review. International J Hepatol 2011, Article ID 104685
10. Minami Y, Kudo M (2013) radiofrequency ablation of liver metastases from colorectal cancer: a literature review. Gut Liver 7(1):1–6
11. Ferras LL, Ford NJ, Morgado ML, Nobrega JM, Rebelo MS (2015) Fractional Pennes bioheat equation: theoretical and numerical studies. Fract Calc Appl Anal 18:1080–1106
12. Facciorusso A, Serviddio G, Muscatiello N (2016) Local ablative treatments for hepatocellular carcinoma: an updated review. World J Gastrointest Pharmacol Ther 7:477
13. Hinshaw JL, Lubner MG, Ziemlewicz TJ, Lee FT Jr, Brace CL (2014) Percutaneous tumor ablation tools: microwave, radiofrequency, or cryoablation what should you use and why? Radiogr Radiolog Soc N Am 34:1344–1362
14. Rathke H, Hamm B, Gttler F, Rathke J, Rump J, Teichgrber U, de Bucourt M (2014) Comparison of four radiofrequency ablation systems at two target volumes in an ex vivo bovine liver model. Diagn Interv Radiol 20:251
15. Bitsch RG, Duex M, Helmberger T, Lubienski A (2006) Effects of vascular perfusion on coagulation size in radiofrequency ablation of ex vivo perfused bovine livers. Invest Radiol 41:422–427
16. Mikhail AS, Negussie AH, Graham C, Mathew M, Wood BJ, Partanen A (2016) Evaluation of a tissue-mimicking thermochromic phantom for radiofrequency ablation. Med Phys 43:4304–4311
17. Negussie AH, Partanen A, Mikhail AS, Xu S, Abi-Jaoudeh N, Maruvada S, Wood BJ (2016) Thermochromic tissue-mimicking phantom for optimisation of thermal tumour ablation. Int J Hyperth 32:239–243
18. Audigier C, Mansi T, Delingette H, Rapaka S, Mihalef V, Carnegie D, Boctor EM, Choti M, Kamen A, Ayache N, Comaniciu D (2015) Efficient lattice Boltzmann solver for patient-specific radiofrequency ablation of hepatic tumors. IEEE Trans Med Imaging 34:1576–1589
19. Kim Y, Audigier C, Dillow A, Cheng A, Boctor EM (2017) Speed of sound estimation for thermal monitoring using an active ultrasound element during liver ablation therapy (conference presentation). Medical imaging 2017: ultrasonic imaging and tomography. In Proceedings 10139:101390F